

## Fast switching and luminance-controlled fringe-field switching liquid crystal device for vehicle display

Jeong Hwan Yoon, Eo Jin Seo, Seung Jae Lee, Young Jin Lim, Hoon Sub Shin, Seong Min Song, Jae-Min Myoung & Seung Hee Lee

To cite this article: Jeong Hwan Yoon, Eo Jin Seo, Seung Jae Lee, Young Jin Lim, Hoon Sub Shin, Seong Min Song, Jae-Min Myoung & Seung Hee Lee (2019) Fast switching and luminance-controlled fringe-field switching liquid crystal device for vehicle display, *Liquid Crystals*, 46:11, 1747-1752, DOI: [10.1080/02678292.2019.1597193](https://doi.org/10.1080/02678292.2019.1597193)

To link to this article: <https://doi.org/10.1080/02678292.2019.1597193>



Published online: 02 Apr 2019.



Submit your article to this journal [↗](#)



Article views: 155



View related articles [↗](#)



View Crossmark data [↗](#)



# Fast switching and luminance-controlled fringe-field switching liquid crystal device for vehicle display

Jeong Hwan Yoon<sup>a\*</sup>, Eo Jin Seo<sup>b\*</sup>, Seung Jae Lee<sup>a</sup>, Young Jin Lim<sup>b</sup>, Hoon Sub Shin<sup>b</sup>, Seong Min Song<sup>b</sup>, Jae-Min Myoung<sup>a</sup> and Seung Hee Lee<sup>b</sup>

<sup>a</sup>Department of Materials Science and Engineering, Yonsei University, Seoul, Korea; <sup>b</sup>Applied Materials Institute for BIN Convergence, Department of BIN Convergence Technology and Department of Polymer Nano Science and Technology, Chonbuk National University, Jeonju, Jeonbuk, Korea

## ABSTRACT

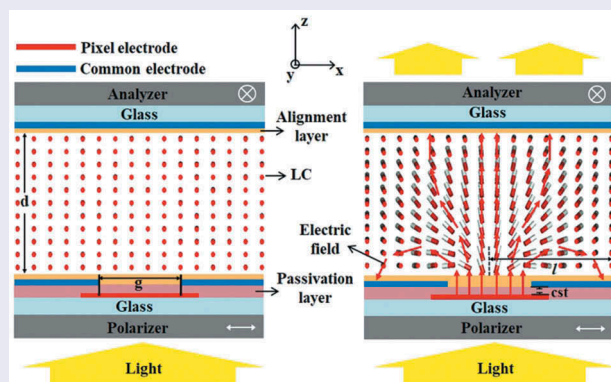
Liquid crystal displays (LCDs) for vehicle displays should exhibit a fast response time in wide temperature range and wide-viewing angle in horizontal and downward directions without grey-scale inversion but limited brightness in the upward direction because the display images can be reproduced in the front window glass of a vehicle, affecting driver's front visibility. Currently, fringe-field switching (FFS) liquid crystal device is widely commercialised for high resolution and wide-viewing-angle LCD; however, it needs to improve response times and limit the display brightness in the upward direction. As a solution, we propose a homogeneously aligned liquid crystal device in which liquid crystal director does tilt as well as twist deformation in a confined area by both vertical- and fringe-electric fields, exhibiting about two times faster decay response time than that of conventional FFS mode with suppressed luminance in the upward direction. The proposed liquid crystal device can be applied to LCDs for vehicle displays.

## ARTICLE HISTORY

Received 6 January 2019  
Accepted 16 March 2019

## KEYWORDS

Fringe-field switching; vehicle display; fast response time; viewing angle



## 1. Introduction

Recently, automobiles and any vehicular displays adopt lots of digital displays for multipurposes, replacing the conventional analogue type of dashboards. Severe competition between two display devices such as liquid crystal displays (LCDs) and organic light-emitting-diodes exists, but each device should overcome its own demerit. One of the demerits in LCDs is relatively slow response, especially at a very low temperature like  $-30^{\circ}\text{C}$  [1,2]. In addition, the displayed images are mirror-reflected at the surface of front glass in vehicle displays, which disturbs

the driver's visibility at night driving. To solve this, a light control film suppressing the luminance in the upward direction is applied to the display panel, which increases cost and decreases brightness in normal direction.

At present, LCDs utilising fringe-field switching (FFS) mode are widely used for the main centre-information-display owing to the high aperture ratio, high transmittance, low operation voltage and touch-screen tolerance although their response time is not fast enough at low temperature [3–5]. But its demerit is overcome by adopting thin cell gap and positive dielectric anisotropic liquid crystals (LCs) with very

low rotational viscosity, reaching maximum slowest grey-to-grey response time of about 300 ms at  $-30^{\circ}\text{C}$ . On the other hand, Iwata et al. proposed vertical alignment (VA) LCD showing slowest decay response time ( $\tau_d$ ) about 120 ms at  $-30^{\circ}\text{C}$  in which both LC's reorientation and relaxation are controlled by field, and Matsushima et al. proposed short-range lurch control (SLC)-in-plane switching (IPS) mode in which the lateral distance  $l$  between the two non-responsive LC regions exists under the applied field such that its response time becomes one-third of conventional FFS mode, showing the slowest  $\tau_d$  about 126 ms at  $-30^{\circ}\text{C}$  [6–9]. In both approaches, response times are greatly improved; however, both suffer from low transmittance and relatively complex driving with two thin-film-transistors in the VA-LCD and fine optimisation of the electrode structure to control LC rotating direction in SLC-IPS LCD are required, respectively.

In this paper, we propose a novel LC device in which LCs are homogeneously aligned initially and driven by both fringe and vertical electric fields formed by one pixel and two common electrodes unlike two electrodes in the conventional FFS device. In voltage-on state, LCs rotate in two opposite directions along a symmetry axis like SLC-IPS but with some tilt angle. Its rotating direction is clearly defined so that it does not require any complex pixel design and driving. The device named luminance-controlled FFS (LC-FFS) shows faster response time than that of

the conventional FFS mode and wide-viewing angle but suppressed luminance in the upward direction.

## 2. Structure and switching principle of LC-FFS device

In a voltage off-state of the LC-FFS device, LC molecules with positive dielectric anisotropy are homogeneously aligned between two substrates under two crossed polarisers with some tilt angle like less than  $5^{\circ}$ , in which the optic axis of the LC director is coincident with one of the polariser axes, as shown in Figure 1(a). In the device, a bottom substrate has two electrode layers: pixel and common transparent electrodes with a passivation layer between them. The common electrode has an open area with some electrode gap ( $g$ ). A top substrate has a plane transparent electrode, but its electrical signal is connected to the bottom common one. In this way, when a bias voltage is applied to the pixel electrode, the vertical ( $E_z$ ) as well as fringe ( $E_z$  and  $E_x$ ) electric field is formed depending on electrode positions; that is, a pure vertical electric field is formed in the open gap, but both fringe and oblique electric fields are formed at both edges of the open gap with its field directions opposite to each other, as shown in Figure 1(b).

The normalised transmitted light ( $T/T_0$ ) of an incident light in which a uniaxial nematic LC medium with

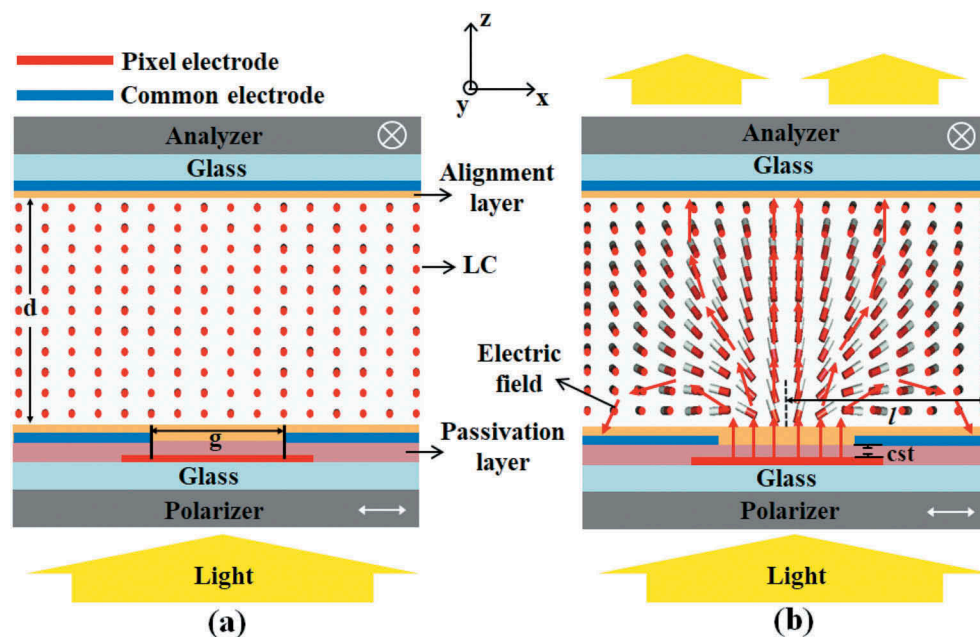


**Figure 1.** (Colour online) Schematic cross-sectional view of the LC-FFS device with LC director and electric field lines in (a) dark and (b) bright state. The red arrows indicate electric field direction between pixel and common electrodes. In the voltage-on state, LC director experiences tilt as well as twist deformation as indicated in Figure 1(b).

its optic axis in plane exists under crossed polarisers is given by

$$\frac{T}{T_0} = \sin^2(2\psi(V))\sin^2\left(\frac{\pi d\Delta n(V)}{\lambda}\right), \quad (1)$$

where  $\psi$  is a voltage-dependent effective angle between the transmission axes of the crossed polarisers and the LC director,  $d$  is the cell gap,  $\Delta n$  is the voltage-dependent effective birefringence of LC and  $\lambda$  is the wavelength of an incident light. In a voltage-off state, the LC-FFS device appears to be a dark state because  $\psi = 0^\circ$ . With bias voltage, the LC director at the centre of the open gap tilts along  $E_z$  so that the transmittance does not occur in this region; however, the LC directors at both left and right edges of the open gap rotate counterclockwise and clockwise, respectively, while the tilt angle of LC directors increases towards the initially given tilt angle, giving rise to a bright state, as indicated in Figure 1(b).

In conventional FFS devices, a rise response time ( $\tau_r$ ) is strongly dependent on applied voltages, and thus, it can be faster by applying a higher voltage. However, a decay response time ( $\tau_d$ ) is associated with the elastic restoring force of LC cell, such that it mainly depends on  $d$  and viscoelastic property of LC, that is,  $\tau_d = \gamma d^2 / \pi^2 K_2$ , where  $\gamma$  is the rotational viscosity and  $K_2$  is twist elastic constant of LCs. For an LC,  $\gamma$  increases exponentially with decreasing temperature so that the slowest grey-to-grey  $\tau_d$  goes easily over 300 ms. In the SLC-IPS mode,  $\tau_d$  is modified into

$$\tau_d = \frac{\gamma}{\pi^2 \left( \frac{K_2}{d^2} + \frac{K_1}{l^2} \right)} \quad (2)$$

In a condition, when  $K_1 = 2K_2$  and  $l = d$ ,  $\tau_{d\text{-SLC}} = \frac{\gamma d^2}{3\pi^2 K_2} = \tau_{d\text{-IPS}} / 3$ , so that the  $\tau_d$  of SLC-IPS mode becomes three times faster than that of the conventional FFS mode, giving rise to fast response times even in low temperature. In the LC-FFS device, the distance  $l$  also exists as defined in Figure 1(b) although the LC above the open gap reorients along  $E_z$  and an elastic deformation of LC director is mainly associated with  $K_2$  although  $K_1$  and bend ( $K_3$ ) deformation involves too. Therefore,  $K_1$  is replaced by  $K_2$  in Equation.(2). As a result, when  $K_1 = 2K_2$  and if  $l = 0.875d$ ,  $\tau_{d\text{-LC-FFS}} = \frac{\gamma d^2}{3.61\pi^2 K_2} \approx \tau_{d\text{-IPS}} / 3.61$ ; that is, the decay response time of the LC-FFS mode can be more than three times faster than that of the conventional FFS mode.

Electro-optics of LC-FFS device can depend mainly on  $g$  because it determines  $l$ , a critical parameter for deciding response time, threshold voltage and transmittance. The proposed device can also be applicable to a high-resolution active matrix LCD with a pitch less than 10  $\mu\text{m}$  or when a pixel pitch is larger than that

two or more number of  $g$ s can exist. Consequently,  $g$  can be determined depending on pixel size and requirements of the electro-optic specification. In addition, noise fields from the data lines can be easily screened by the common electrode above pixel and by designing a pixel electrode size larger than the open gap size, and a storage capacitor ( $C_{st}$ ) is automatically formed between pixel and common electrode without sacrificing an aperture ratio (see Figure 1(b)), which allows the device to realise high aperture without an optical crosstalk in active matrix LCDs [10,11].

### 3. Results and discussion

To investigate electro-optic characteristics of the LC-FFS device, a numerical simulation was done by a well-known commercialised multi-dimensional finite element method (FEM) solver (TechWiz LCD, Sanayi system). The distribution of electric potential was calculated by Laplace's equation, and the optical transmittance was generated based on the  $[2 \times 2]$  extended Jones matrix method. To understand field-response of LC directors and its corresponding transmittance, common electrode structures with three different open gaps ( $g$ s) of 1, 2 and 3  $\mu\text{m}$  on a bottom substrate were evaluated and the thickness of passivation layer between pixel and common electrodes was 300 nm. The physical properties of LCs tested are as follows: dielectric anisotropy  $\Delta\epsilon = 8.2$ , birefringence  $\Delta n = 0.1148$  at 550 nm, rotational viscosity  $\gamma = 80$  mPa-s,  $K_1/K_2/K_3 = 16.9/8.42/19.2$  in pN and the  $d$  is 4  $\mu\text{m}$ . The surface pretilt angle is to the  $y$  direction is  $1^\circ$ .

At first, voltage-dependent transmittance curves were measured for three different  $g$ s, as shown in Figure 2(a). As the size of  $g$  increases, both threshold and operating voltages decrease, indicating that its switching behaviour strongly depends on  $g$ . But, the average transmittance saturates at  $g = 2 \mu\text{m}$  and does not increase further with increasing  $g$  to 3  $\mu\text{m}$ . Next, the electrode-position-dependent transmittance was investigated along a horizontal direction for three different  $g$ s at three different voltages, as shown in Figure 2(b). As expected, the transmittance does not occur at the centre of  $g$ s because  $\psi$  keeps  $0^\circ$  although the LC director reorients along the  $E_z$ ; however, it occurs at both edges of the open gap. The induced maximum transmittance in two lobes of transmittance profile increases when  $g$  increases from 1 to 2  $\mu\text{m}$  but saturates at  $g = 3 \mu\text{m}$ . In the switching principle, we claim that the LC directors at left and right edge of the gap will rotate anticlockwise and clockwise with increased tilt angle, respectively, and as a proof, the LC director profile was calculated in LC-FFS with  $g = 3 \mu\text{m}$ , especially at two electrode positions which gives maximum transmittance

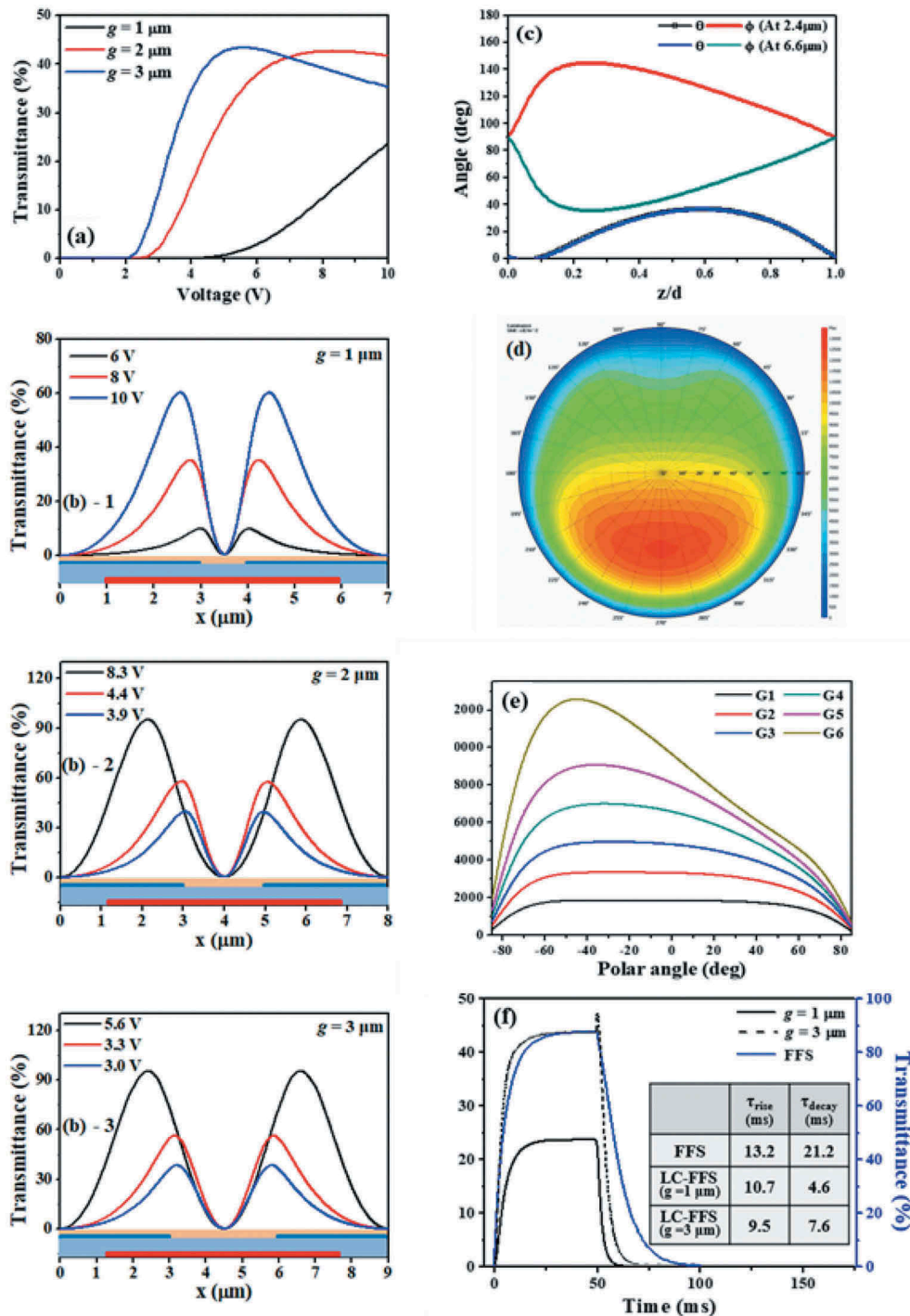


**Figure 2.** (Colour online) Calculated (a) voltage-dependent transmittances at three different  $g$ s, (b) electrode-position-dependent transmittances at three different voltages when  $g$  is 1, 2 and 3  $\mu\text{m}$  in the LC-FFS cell, (c) LC director profile in twist and tilt angle at the electrode position with maximum transmittance at 5.6 V when  $g = 3 \mu\text{m}$ , (d) iso-luminance contour in the white state, (e) luminance change at 6 grey scales along vertical direction, and (f) time-dependent transmittance curves in the FFS and LC-FFS cells in which the electrode width and gap between patterned electrodes in the FFS device are 3 and 4.5  $\mu\text{m}$ , respectively. In calculating (d) and (e), the retardation of the cell is tuned to be 0.326  $\mu\text{m}$ . The transmittance is normalised to two parallel polarisers.

as indicated in Figure 2(c). The initial pretilt angle  $1^\circ$  increases to  $36.5^\circ$  at  $z/d = 0.6$ , while the twisted angle at  $x = 2.4$  and  $6.6 \mu\text{m}$  is  $54.7^\circ$  and  $-54.7^\circ$ , respectively, at  $z/d = 0.25$ , indicating that the transmittance in upward and

downward directions can be asymmetric and the LC directors at both edges of the gap rotate in opposite directions each other. In addition, the transmittance in the upward direction is lower than that at normal direction due to



reduced effective retardation associated with generated high tilt angle towards upward direction. Figure 2(d,e) shows iso-luminance contour in white state and luminance change according to vertical viewing directions at 6 different grey scales of LC-FFS cell. As clearly indicated, the luminance in the white state at normal direction decreases by 36.4% and increases by 29.8% along upward and downward viewing directions at a polar angle of  $40^\circ$ , respectively, while the lower the grey scales, the asymmetry becomes smaller due to smaller tilt angle at lower grey scales. Conclusively speaking, high image quality without grey scale inversion while suppressing the luminance in the upward direction is achieved. Response times between LC-FFS and FFS devices are compared, as shown in Figure 2(e). Since both modes use the same LC and cell gap, its response behaviour is purely determined by intrinsic device characteristics. Rise response times ( $\tau_{r,s}$ ) of FFS and LC-FFS ( $g = 1 \mu\text{m}$ ) devices are 13.2 and 10.7 ms, respectively, such that about 19% becomes shorter in the LC-FFS device. Very impressively, the  $\tau_d$  of the LC-FFS device becomes veryfast such that 21.1 ms in the FFS device is reduced to 4.6 ms, that is, about 4.6 times becomes faster. In this case,  $K_1 = 2K_2$  and  $l$  is  $3.5 \mu\text{m}$  ( $l/d = 0.875$ ), so that  $\tau_{d\text{-LC-FFS}} \cong \tau_{d\text{-IPS}}/3.6$ , which is quite

clear that the fast response of the LC-FFS device originates from short distance of nonresponsive LC region. When  $g = 3 \mu\text{m}$ , the  $\tau_d$  of the LC-FFS device is 7.6 ms, which is about 2.8 times faster than that of the FFS device. In this case,  $l = 4.5 \mu\text{m}$  ( $l/d \cong 1.1$ ), then  $\tau_{d\text{-LC-FFS}} \cong \tau_{d\text{-IPS}}/2.6$ , indicating that the theoretically estimated value shows reasonable value.

Both LC-FFS and conventional FFS devices were fabricated using the LC with similar physical properties given above to confirm the switching principle and shortened decay time of the proposed device. In the experimental cells, normal FFS electrode structure was tested for both cells, in which  $g$  and width of the patterned common electrode was 4.5 and  $3 \mu\text{m}$ , respectively, and the cell gap was  $3 \mu\text{m}$  because thin cell gap is generally applied for achieving fast response time in the FFS mode. The physical properties of LCs used in the experiment are as follows:  $\Delta\epsilon = 8.0$ ,  $\Delta n = 0.1088$  at  $589 \text{ nm}$ ,  $\gamma = 81 \text{ mPa}\cdot\text{s}$ ,  $K_1/K_2/K_3 = 18.3/8.42/17.7$  in pN. Figure 3 shows the measured electro-optic characteristics of LC-FFS and FFS devices using LCMS-200 (Sesim Photonics Technology Inc., South Korea). The measured voltage-dependent transmittance curves show that both devices exhibit about the same threshold voltage; however, the operating voltage at which maximum transmittance occurs is 5.4 and 4.8 V in

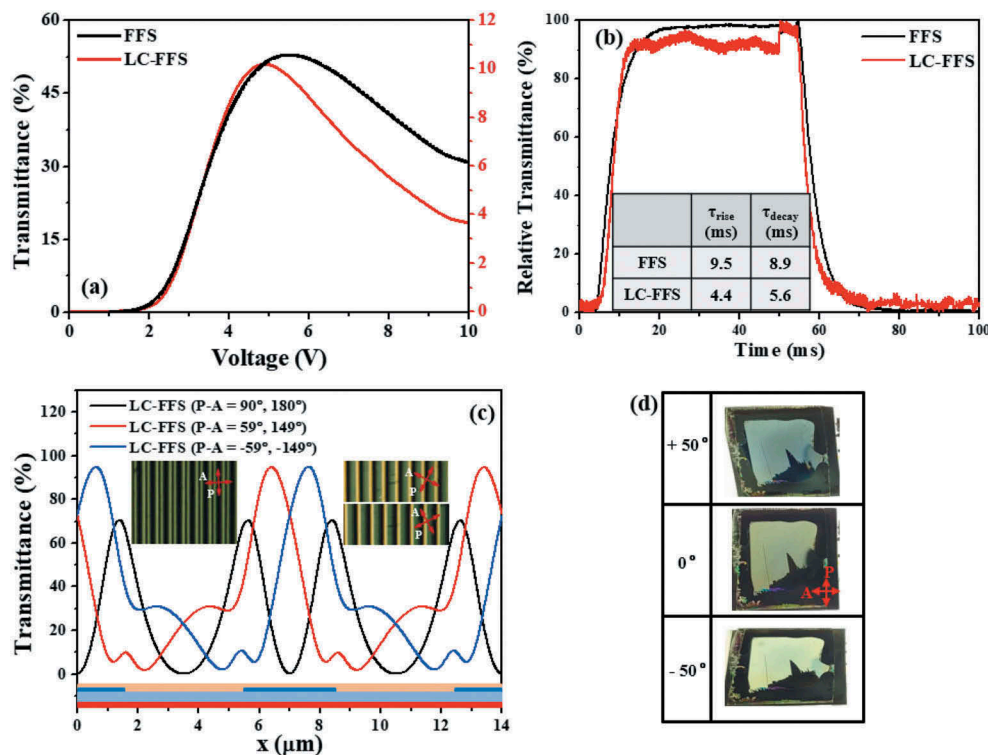


**Figure 3.** (Colour online) Measured (a) voltage-dependent and (b) time-dependent transmittance curves between FFS and LC-FFS devices. (c) POM images of the LC-FFS in a dark and bright state. In addition, the rotation of the crossed polarisers breaks the transmittance symmetry in stripes as indicated in the calculated results. (d) Macroscopic images of the LC-FFS showing the luminance change when the cell is tilted in the upper and lower direction. In the FFS, the initial LC director makes an angle of  $10^\circ$  with respect to the electrode direction with a pretilt angle of  $2^\circ$ .

FFS and LC-FFS devices, respectively; that is, the operating voltage decreases, but the transmittance loss occurs compared to the FFS device as shown in Figure 3(a). We have also observed the polarizing optical microscopy (POM) images in the white state of LC-FFS device in which the transmittance at both edges of the open gap occurs in stripe pattern, while the centre of the open gap remains a dark state, as can be seen in Figure 3(c). To confirm the LC directors at left and right edges rotate anticlockwise and clockwise, respectively, the crossed polarisers rotate anticlockwise and clockwise and the resultant transmittance texture breaks symmetry such that the brightness in left (right) stripe decreases (increases) when it was rotated anticlockwise. The calculated transmittance along  $x$  direction while rotating the crossed polariser clearly proves it. Figure 3(b) shows the measured response times of LC-FFS and FFS devices. The  $\tau_r$  and  $\tau_d$  of LC-FFS (FFS) device are 4.4 (9.5) ms and 5.6 (8.9) ms, respectively. The  $\tau_r$  and  $\tau_d$  of the LC-FFS device are about 2.2 and 1.6 times faster than those of the FFS device. In the given experiments,  $l$  is 3.75  $\mu\text{m}$ , which is larger than  $d$ , so that the reduction effect on  $\tau_d$  decreases compared to the calculated result. Utilising Equation (2) and parameter conditions like  $l/d = 1.25$ ,  $K_1 \cong 2.17K_2$ ,  $\tau_{d\text{-LC-FFS}} \cong \tau_{d\text{-IPS}}/2.3$  in which the measured value is slightly smaller than the estimated one.

#### 4. Conclusion

We have proposed fast switching and luminance-controlled homogenous alignment LCD with the use of a positive dielectric anisotropy LC for vehicular centre-information-display. Compared to main commercialised FFS display for this purpose, the proposed device shows faster response time than that of the FFS mode, which is favoured for low temperature operation, and suppressed and enhanced luminance in the upward and downward directions by the device itself compared to that at normal direction which decreases image reflection to the front mirror of the vehicle while keeping high image quality without showing grey scale inversion. We expect the proposed device has a strong potential to be applicable for not only vehicular displays but also application displays like aeroplane in which the luminance in the upward direction requires to be suppressed.

#### Disclosure statement

No potential conflict of interest was reported by the authors.

#### Funding

This research was supported by the Basic Science Research Program (2016R1D1A1B01007189) through the National Research Foundation of Korea (NRF) funded by Ministry of Education.

#### References

- [1] Mizusaki M, Tsuchiya H, Minoura K, et al. High performance fringe field switching mode liquid crystal display with photo-alignment technology for vehicular application. *SID Symp Dig Tech Pap.* 2018;49:351–354.
- [2] Chen H, Peng F, Gou F, et al. Nematic LCD with motion picture response time comparable to organic LEDs. *Optica.* 2016;3(9):1033–1034.
- [3] Lee SH, Lee SL, Kim HY. Electro-optic characteristics and switching principle of a nematic liquid crystal cell controlled by fringe-field switching. *Appl Phys Lett.* 1998;73:2881.
- [4] Kim MS, Ham HG, Choi H-S, et al. Flexoelectric in-plane switching (IPS) mode with ultra-high-transmittance, low-voltage, low-frequency, and a flicker-free image. *Opt Express.* 2017;25:5962.
- [5] Kim MS, Jin HS, Lee SJ, et al. Liquid crystals for superior electro-optic performance display device with power-saving mode. *Adv Opt Mater.* 2018;6:1800022.
- [6] Peng F, Huang Y, Gou F, et al. High performance liquid crystals for vehicular displays. *SID Symp Dig Tech Pap.* 2016;47:754–757.
- [7] Mastushima T, Okazaki K, Yang Y, et al. New fast response time in-plane switching liquid crystal mode. *SID Symp Dig Tech Pap.* 2015;46:648–651.
- [8] Matsushima T, Seki K, Kimura S, et al. Optimal fast-response LCD for high-definition virtual reality head mounted display. *SID Symp Dig Tech Pap.* 2018;49:667–670.
- [9] Iwata Y, Murata M, Tanaka K, et al. Novel super-fast-response, ultra-wide temperature range VA-LCD. *SID Symp Dig Tech Pap.* 2013;44:431–434.
- [10] Ono K, Hiyama I. The latest IPS pixel structure suitable for high resolution LCDs. *Proceeding of the 19th International Display Workshops in conjunction with Asia Display.* Kyoto, Japan: Society for Information Display; 2012: 933–936.
- [11] Yoon JH, Lee SJ, Lim YJ, et al. Fast switching high contrast and high resolution liquid crystal device for virtual reality display. *Opt Express.* 2018;26:34142–34149.